
ELSEVIER

Nuclear Instruments and Methods in Physics Research B 142 (1998) 377–386

NIM B
Beam Interactions with Materials & Atoms

A round robin experiment of elemental sensitivity factors in low-energy ion scattering

H.H. Brongersma [a], M. Carrere-Fontaine [a], R. Cortenraad [a], A.W. Denier van der Gon [a], P.J. Scanlon [a], I. Spolveri [b], B. Cortigiani [b], U. Bardi [b], E. Taglauer [c], S. Reiter [c], S. Labich [c], P. Bertrand [d], L. Houssiau [d], S. Speller [e], S. Parascandola [e], H. Ünlü-Lachnitt [e], W. Heiland [e,*]

[a] *Faculty of Physics, TU Eindhoven, P.O. Box 513, NL-5600 MB Eindhoven, The Netherlands*
[b] *Dipartimento di Chimica, Universita di Firenze, I-50121 Firenze, Italy*
[c] *Max-Planck-Institut für Plasmaphysik, D-85748 Garching, Germany*
[d] *Universite Catholique de Louvain, PCPM, 1 Place Croix du Sud, B-1348 Louvain-la-Neuve, Belgium*
[e] *Fachbereich Physik, Universität Osnabrück, D-38023 Osnabrück, Germany*

Received 30 January 1998; received in revised form 16 March 1998

Abstract

In a round robin experiment a set of five polycrystalline, metallic samples is studied by low-energy ion scattering (LEIS) in five different laboratories. The energy range is 0.6–3.5 keV and He and Ne ions are used. Even though different experimental setups are used the evaluated elemental sensitivity factors agree within ±20%. Reproducibility within single laboratories is better than 10%. In an additional study carried out in three laboratories the surface composition of an alloy, $Cu_{55}Pd_{45}$, was determined, using in situ calibration standards. These surface composition measurements agreed within ±3 at% demonstrating that quantitative composition determination is possible using this procedure.

Keywords: Low-energy ion scattering; LEIS; Ion-solid interactions; Surface analysis

1. Introduction

Low-energy ion scattering (LEIS or ISS) has found many applications in compositional surface analysis and surface structure analysis [1–4]. One of the goals of any given surface analytical technique is the quantitative analysis. In the case of LEIS this goal is of special interest because LEIS has the ultimate surface sensitivity compared to other composition analysis techniques, such us X-ray photoelectron spectroscopy (XPS), Auger electron spectroscopy (AES) or secondary ion mass spectroscopy (SIMS), to name the most common surface analytical tools. The quantitative

* Corresponding author. Tel.: +49 541 9690; fax: +49 541 969 2670; e-mail: wheiland@dosuni1.bitnet.

0168-583X/98/$19.00
PII: S0168-583X(98)00264-X

capability of these techniques decreases in the order of XPS, AES and SIMS. There are many reasons for this state of art. XPS faces a background problem due to elementary excitations and hence losses of the exiting photoelectrons, however, the physics involved is well understood. Therefore the background subtraction procedure is quantitatively established and is part of commercial XPS software packages. Nevertheless, the depth resolution of XPS is limited, due to the escape depth of the photoelectrons of several atomic layers [5]. In AES the spectral lines of the Auger-electrons are in general at low kinetic energies sitting on a background of 'true' secondary electrons. The treatment of this background is at present less quantitative compared to the XPS case, where the background problem is less severe [5,6].

SIMS for quantitative analysis faces two problems, the destruction of the surface and the emission of polyatomic species. A particular problem is the ion yield of the sputtered particles, which depends on the 'chemical' environment of the surface. Nevertheless, there are several techniques available to overcome these problems at least in special cases which afford quantitative SIMS analysis using the proper calibration [7,8].

LEIS, from the point of view of quantitative elemental analysis, faces a neutralisation problem. It is well established that the ion survival probabilities of rare gas ions scattered from surface atoms are very low, of the order of a few percent at most, and the survival of ions scattered from second layer atoms is essentially zero. This effect makes LEIS very surface sensitive. So far, in contrast to the 'matrix effect' in SIMS, only few cases are known for a dependence of the ion survival probability of scattered ions on the chemical composition of the surface. This finding is true only for large impact and scattering angles. At grazing angles, the scattering and the neutralisation are influenced by neighbouring atoms naturally. In this work a round robin experiment is described to establish sensitivity factors for elemental metal targets comparing results from five different laboratories. For the results presented here impact angles from 45° up to perpendicular incidence have been used. The energy spectra of the scattered ions are measured by using electrostatic analysers, i.e. electrostatic prisms and cylindrical mirror analysers (CMA). This implies scattering angles of 90° and approximately 140°. The results of the five different laboratories show reasonable agreement in most cases, but there are large, non-systematic discrepancies which are presently not understood.

2. Experiment

Three of the five laboratories use CMAs, two of which use perpendicular incidence of the ions (Eindhoven [9] and Louvain [10]). Garching [11] uses a CMA and an impact angle of 60° relative to the surface. Firenze [12] has a hemispherical electrostatic analyser at a scattering angle of 135°, very close to the scattering angles of the CMAs of 142, 139 and 137° of Eindhoven, Louvain and Garching, respectively. The impact angle in Firenze is 68°. In Osnabrück [13] the LEIS spectra are measured with a spherical electrostatic analyser at 90° and at an impact angle of 45°.

The ion beam systems are quite different in the five laboratories. Only Osnabrück and Eindhoven apply a magnetically analysed beam, the others make up for this deficiency of not having mass analysis by running isotopically clean primary gas in the ion source. The gases are ^{3}He, ^{4}He, natural Ne and ^{20}Ne. The energy range is 0.5–3.5 keV. The experimental parameters are listed in Table 1.

The targets analysed in this study are high purity, polycrystalline Al, Ni, Cu, Pd and Pt samples from the same respective batch. The samples were cleaned in all cases by low energy (1–3 keV) Ar or Ne ion beams (Table 2.). Base pressures in all experimental systems are in the 10^{-9} mbar range or better. Major cleaning or impurity problems are observed with Al and Pd, i.e. Al needed up to 100 h sputtering at 100 nA of primary beam current scanned over an area of 10×10 mm^2.

The measured spectra are evaluated following established formulas. The LEIS intensity (ions) of ions scattered from atoms i of the target is given by

$$Y_i = I_p\, n_i\, \sigma_i\, P_i^+ RT = I_p\, \eta_i\, c_i, \qquad (1)$$

where I_p, the primary beam current (ions); n_i, the number of surface atoms of element i per unit surface area; σ_i, the differential scattering cross

Table 1
Experimental parameters of the LEIS systems used in the five laboratories. CMA is a cylindrical mirror analyser, hemisph. is short for an hemispherical electrostatic analyser and ESA stands for a 90° spherical electrostatic analyser. Ψ is the angle of incidence measured against the surface plane, Θ is the laboratory scattering angle

Key	Lab	Detector	Type	Post acc.	e^-suppr.	θ	Θ	Projectiles	Energy (keV)
*g*1	Eindhoven	CMA	Ch.tron	*n*	bias	90°	142°	$^3He^+$,$^4He^+$,$^{20}Ne^+$	0.6, 1, 1.5, 2, 2.5, 3, 3.5
*g*2	Firenze	hemisph [a]	Ch.tron	*n*	Faraday C	68°	135°	$^4He^+$	0.8, 1, 1.5, 2
*g*3	Garching	CMA	Ch.tron	3 keV	Faraday C	60°	137°	$^4He^+$	0.5, 1, 2
*g*4	Louvain	CMA	Ch.tron	*n*	Faraday C	90°	139°	$^3He^+$	1, 2, 3
*g*5	Osnabrück	ESA	Ch.plate	2 keV	n	45°	90°	$^4He^+$,$^{20}Ne^+$	1, 2, 3

[a] Fixed path energy, 90 eV.

section for the scattering by the element i and for the chosen scattering angle; P_i^+, the ion survival probability for the scattering from atoms i; R, a factor, taking into account the roughness of the surface [14], we assume R to be equal for all samples; T, the transmission of the analyser including the solid angle of detection (sr) and the detection efficiency; η_i, the sensitivity factor of element i relative to Cu; c_i, the relative surface concentration (surface coverage in parts of a Cu monolayer) of element i.

In the laboratories involved (with the exception of Louvain), the ions are postaccelerated, such that the detection sensitivity is independent of the scattering energy. The solid angles of detection vary considerably among the different analysers between 0.12 sr [9] and 3×10^{-4} sr [13]. Consequently, the count rate or the intensity/charge (counts/nC) also varies among the different laboratories. Nevertheless good agreement is found for these yields, e.g. for 2 keV $^4He^+$ scattered off Cu the yield is 35×10^3 (counts/nC sr). Therefore, all data are normalised to the yield of He^+ off Cu at 2 keV, i.e. the system He^+/Cu is used as the calibration standard.

3. Results

The basic results of the ion scattering experiments are doubly differential energy spectra. Fig. 1 shows a set of spectra for He^+/Ni for the energy range of 0.5–3.5 keV from Eindhoven. The peak position for each primary energy E_0 can be deduced from the binary collision formula which is obtained from considering conservation of energy and momentum

$$E_f/E_0 = (1 + M_2/M_1)^{-1}(\cos\Theta + [(M_2/M_1)^2 - \sin^2\Theta]^{1/2})^2. \quad (2)$$

Here M_2 is the target atom mass and M_1 is the projectile atom mass. Θ is the laboratory scattering angle. For a scattering angle of 90° the equation is simplified to

$$E_f/E_0 = (M_2 - M_1)/(M_2 + M_1). \quad (3)$$

Table 2
Experimental parameters describing the target cleaning procedures used in the five laboratories

Lab	Pressure range	Projectile	Energy	Angle	Annealing	O_2	Beam diameter	Curr
*g*1	10^{-9} mbar	Ar^+	3 keV	90°	*n*	*y*	5 mm	160 nA
*g*2	10^{-9} mbar	Ar^+	2 keV	90°	*n*	*n*	10 mm	500 nA
*g*3	10^{-7} (rare gas)							
*g*4	10^{-9} mbar	Ar^+	2 keV	90°	*n*	*n*	1 mm (scan 10 mm)	50 nA
*g*5	10^{-9} mbar	Ne^+	2 keV	30°	*n*	*n*	1 mm (scan 10 mm)	100 nA

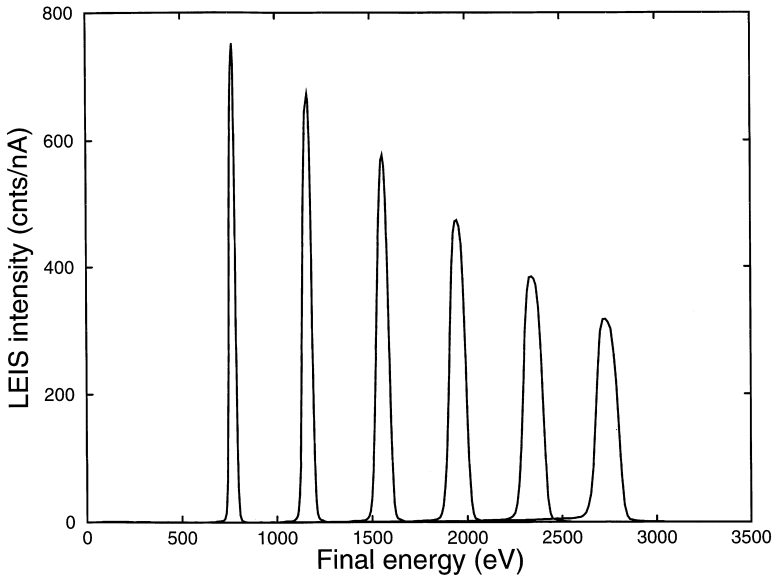

Fig. 1. Ion energy spectra of $^4He^+$ scattered from polycrystalline Ni at a scattering angle of 142°. The incident ion beam direction is perpendicular to the target surface. The primary energies are 0.5, 1.0, 1.5, 2.0, 2.5, 3.0 and 3.5 keV from left to right (Eindhoven).

The peaks in the spectra are almost of gaussian shape, the width increases with the primary energy. When the yields are normalized to the same relative height and plotted vs. the relative energy, E_f/E_0, the spectra coincide. The low-energy tail in the spectra at higher primary energies is due to ions scattered from the second and deeper layers, showing that at these energies the ion survival or reionizition probability for scattering from deeper layers increases. For a primary energy of 2 keV this effect is marginal for many target materials, another good reason to choose 2 keV for calibration. It is obvious that at 3.5 keV primary energy the low energy tail extends into the peak area and hence poses a background subtraction problem. The envelope of the peak heights of the spectra qualitatively follows the expected behaviour, i.e. since the differential scattering cross section increases with decreasing energy and the ion survival probability decreases with decreasing energy, the product ofthese two factors in formula (1) causes the shape of the envelope.

In Fig. 2 we show Osnabrück data of the cleaning procedure of Al by 2 keV Ne sputtering at an angle of incidence of 30° with a beam current of 100 nA scanned over an area of $10 \times 10\,mm^2$. The total sputter time was 120 h. The evidence for the O-peak at $0.6\,E_0 = 1200$ eV for a 2 keV primary He beam is vanishing but a low energy tail remains. The ion yield at the lowest energies is due to sputtered ions. The results from the other laboratories are comparable. At energies as low as 1000 eV the low energy tail becomes tolerably small in the case of He^+/Al. This effect is due to the lower Z of Al, which causes lower scattering cross sections and hence a larger penetration depth of the primary He^+ ions. Furthermore He^+ ions that have been neutralized, can be reionized during a strong interaction with an Al atom. Thresholds for this process have been determined [15]. These thresholds (300 eV for He^+ on Al) dictate the onset of the low-energy tails in the energy spectra.

In Table 3, the experimental intensity ratios from each of the participating laboratories are collected. The laboratory label is as in Table 1. In each case the ratios are given relative to the 2 keV $^4He^+$/Cu yield of the respective laboratory. The intensity ratios are calculated from the peak heights $S_{j,e}$ (counts/nC) of element j at energy e relative to the peak height of Cu at 2 keV. The different target atom density is taken into account by the ratio of the respective atom densities of the

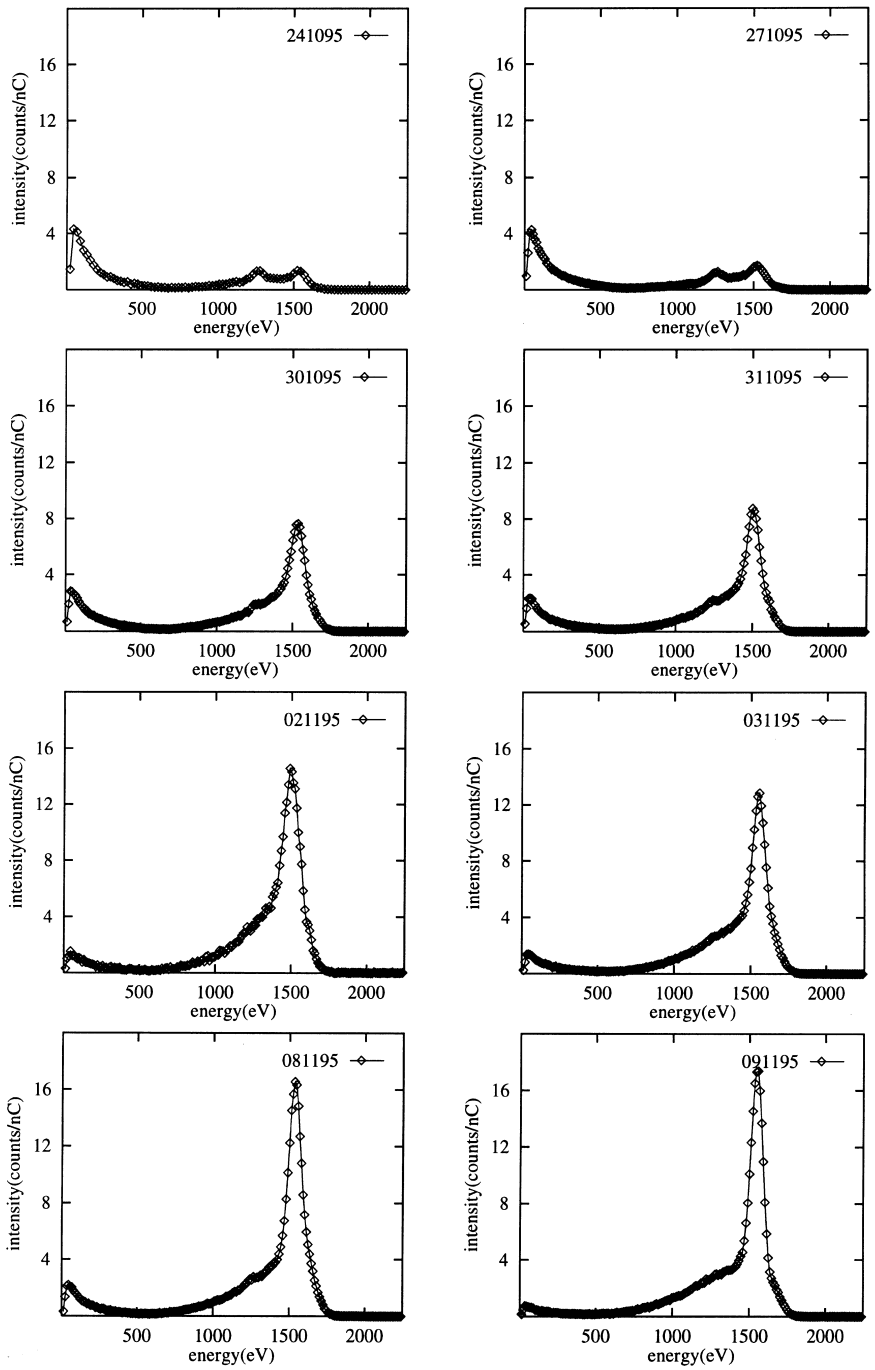

Fig. 2. Ion energy spectra of 2.02 keV $^4He^+$ scattered from Al at a scattering angle of 90°. The angle of incidence is 45°. The continuous cleaning of the target by Ne sputtering is monitored by the decrease of the O-peak at 1200 eV and the increase of the Al peak at 1480 eV. The total sputter time with a beam current of 100 nA and at an angle of incidence of 30° is 120 h. The beam is scanned over an area of $10 \times 10\ mm^2$ on the target surface (Osnabrück). The data have not been corrected for the transmission of the analyser. The ion fluence between subsequent spectra is approximately $60\ \mu C/cm^2$.

Table 3
Relative intensities (relative to He^+/Cu and Ne^+/Cu at 2 keV) of $^4He^+$ and Ne^+ scattering from Ni, Cu, Pd and Pt

Energy keV	$g1$	$g2$	$g3$	$g4$	g5
He/Ni					
1.0	1.02	1.87	2.71	0.67	0.97
2.0	0.48	0.49	0.50	0.33	0.48
3.0	0.33			0.24	0.32
He/Cu					
1.0	2.16	2.66	4.9	1.69	2.66
2.0	1.00	1.00	1.00	1.00	1.00
3.0	0.61			0.62	0.49
He/Pd					
1.0	0.85	0.85	2.24	0.37	1.00
2.0	0.37	0.19		0.31	0.29
3.0	0.29			0.22	0.19
He/Pt					
1.0	0.55	0.87	1.05	0.53	0.68
2.0	0.31	0.24		0.38	0.34
3.0	0.21			0.17	0.19
Ne/Ni					
1.0	1.02				1.02
2.0	0.44				0.35
3.0	0.32				0.21
Ne/Cu					
1.0	2.76	8.32			5.15
2.0	1.00	1.00			1.00
3.0	0.50				0.60
Ne/Pd					
1.0	0.21				0.34
2.0	0.08				0.15
3.0	0.12				0.25
Ne/Pt					
1.0	0.36	0.72			1.55
2.0	0.16	0.15			0.54
3.0	0.10				0.46

(1 1 1) surfaces of the materials n_{cu}/n_j. For the Osnabrück data also the differential scattering cross section ratios are taken into account, because of the different scattering angle used (Table 1). The intensity ratios $r_{j,e}$ are

$$r_{j,e} = \frac{S_{j,e}}{S_{Cu,2\ keV}} \cdot \frac{n_{cu}}{n_j} \cdot \frac{E_{f,Cu,2\ keV}}{E_{f,j,e}}, \quad (4)$$

where the E factor (the index f is for final energy of the ion) takes the difference in transmission of the energy analysers into account. This factor is not needed for the Firenze data, since there the analyser is used with constant pass energy (Table 1).

Listed are the values for three energies because for those we have most of the data. Good agreement is found between $g1, g2$ and $g5$ with the exceptions of the cases of Ne^+/Cu and Ne^+/Pt, respectively. In the Ne^+/Cu case the $g2$ data are higher than the $g1$ and $g5$ data. In the Ne^+/Pt case the $g5$ data are by a factor of 3–4 higher than the $g1$ data. In the case of the $g4$ data it is always the 1 keV data point which is consistently lower than the 2 and 3 keV points in comparison to both, $g1$ and $g5$. In the case of He^+/Ni multiplying the $g4$ data by 1.3 leads to a very satisfactory agreement with the $g1$ and $g5$ data. We have no explanation for this factor 1.3. It is a situation comparable to the Ne^+/Pt case where some factor, 3–4, also brings agreement between $g1$ and $g5$. All the $g3$ values are consistently higher by about a factor of 2.0–2.5, only in the case of 2 keV He^+/Ni the value agrees with $g1, g4$ and $g5$, an unexplained finding as well. Within each single laboratory the reproducibility is better than 10%. So each laboratory can establish its own calibration with satisfactory accuracy. Comparing the results with previous data, the Osnabrück group reported a factor of 2 difference for He^+/Ni, the Garching group a relative increase of the Pd and Pt yields compared to the data of 1980 [2,16]. In Fig. 3 the new data are compared with the Garching data of 1985 [16]. Here the relative peak heights are plotted

$$t_{j,e} = \frac{S_{j,e}}{S_{cu,2\ keV}} \cdot \frac{(\sigma_{j,e})_{\theta=140^\circ}}{(\sigma_{j,e})_{\theta=90^\circ}}. \quad (5)$$

The correction for the cross section is needed for the Osnabrück data only.

In Table 4 the resulting sensitivity factors are calculated using Eq. (1) but for relative values only. All data are relative to the He^+/Cu and the Ne^+/Cu values at each given energy. There are no data for Ne^+/Al, because as can be seen from Eqs. (2) and (3), Ne^+ is scattered into large angles by Al at very low energies. At such low energies the transmission of the analysers used is very low. For the numbers of surface atoms, n,

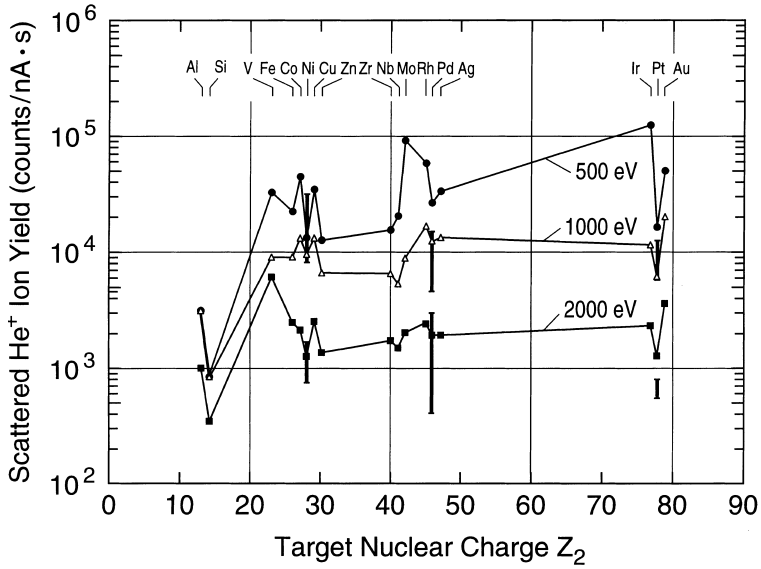

Fig. 3. Comparison of the yields of $^4He^+$ from different targets at 500 eV, 1000 eV, and 2000 eV with data from 1985 [16]. The data are shown as vertical bars, the length of which shows the scatter of the data from different laboratories.

the atomic density of atoms of the respective (1 1 1) faces of the metals are used. The cross sections, σ, are calculated from the Ziegler–Biersack–Littmark potential (ZBL) [1]. The dependence of the analyzer transmission on energy $1/E$ is taken into account. The roughness factor R is assumed to be constant. The error margins are the result of averaging at most five data, so they are rather a measure of the reproducibility of the sensitivity factors than of their accuracy. The scatter of the data discussed for the data of Table 3 is transferred into the data of Table 4. In general, the sensitivity factors increase with increasing primary energy for Al, Ni, Pd and Pt always relative to Cu. The sensitivity factors increase with increasing Z from Al to Pd, but decrease again for Pt. This finding is valid for the He isotopes, but not for Ne. In the case of Ne the sensitivity factor increases continuously with Z. For ^3He the data at 1 keV for Ni, Pd and Pt appear to be systematically too high. For ^4He and Ne the data at 500 or 600 eV show a somewhat erratic behaviour compared to the trend of the energy dependence at higher energies. A rather simple explanation for these findings at the lowest energies may be an experimental problem: focusing of the ion beam is in general more difficult at the lower energies, or the beam size on the target changes relative to the target area 'seen' by the detector. As long as the beam spot is smaller than the area seen by the detector, focusing is no problem. But if the beam size is larger than the area seen by the detector, the signal will depend on the focusing (or the current density). Since only the current and not the current density is measured by a Faraday cup or by measuring the target current, problems arise when evaluating counts/nC. At the lowest energy not all possible neutralization channels are fully understood such that the observed 'trend' could be caused by changes of the relative ion survival or reionization probabilities. This possibility has been discussed before [1–4,14–17]. The encouraging finding is that in the good cases in the energy range around 2 keV the reproducibility can be as good as 10% and is around 20% in a gross average.

The results presented above show that composition determination using sensitivity factors as determined in another experimental setup will give an average accuracy of $\pm 20\%$, but may also produce results which are not better than within a factor of 2. To obtain a better accuracy, a different approach is needed. In a further set of experiments

Table 4
Elemental sensitivity factors for $^3He^+$, $^4He^+$ and Ne^+ for all targets (including Al) and energies included in the study. The elemental sensitivity factor is defined by Eq. (1). The elemental sensitivity factors are normalized to Cu at each energy. The average error is calculated as $\pm\langle(\eta - \langle\eta\rangle)^2\rangle^{1/2}$ and is ±20%

E(keV)	η_{Al}	η_{Ni}	η_{Pd}	η_{Pt}
Primary ion ^3He				
0.5				
1.0	0.22	0.68	1.49	1.10
1.5	0.26	0.57	0.96	1.03
2.0	0.32	0.60	1.00	1.19
2.5	0.45	0.62	1.05	1.19
3.0	0.62	0.72	1.20	1.37
3.5	0.78	0.89	1.51	1.48
Primary ion ^4He				
0.5		0.34	3.21	0.19
1.0	0.27	0.48	1.43	1.23
1.5	0.32	0.48	1.05	1.39
2.0	0.93	0.57	1.14	1.32
2.5	0.53	0.46	1.22	1.31
3.0	0.40	0.78	1.27	1.43
3.5	0.73	0.63	1.53	1.68
Primary ion ^{20}Ne				
0.5				
1.0		0.87	1.14	2.45
1.5		1.09	0.89	1.78
2.0		0.84	0.97	2.59
2.5		0.10	0.92	1.80
3.0		0.90	1.96	3.71
3.5		1.15	1.58	

we tested the use of in situ calibration samples measured under identical conditions as the sample under investigation. For this purpose the surface composition of a $Cu_{55}Pd_{45}$ alloy sample was determined by three groups. Prior to analysis, the sample was sputter-cleaned at room temperature using 2 keV Ar^+ ions. Subsequently, surface composition measurements were performed using $^4He^+$ ion scattering at various energies. The pure Pd and Cu reference samples were measured under identical conditions, also after sputter-cleaning at room temperature. The resulting surface compositions are shown in Table 5. From these results it follows that the composition determinations agree within ±3 at%. It is worth mentioning that a XPS analysis at Garching gave 53.4 at% Cu compared

Table 5
Determination of the surface composition of $Cu_{55}Pd_{45}$ alloy in three laboratories using in situ Cu and Pd polycrystalline samples for calibration. The average result is 58 ± 3 at% Cu

E (eV)	Eindhoven (at% Cu)	Firenze (at% Cu)	Garching (at% Cu)
500			55
1000	58	64	54
2000	56	61	
3000	58		

to the average 58 ± 3 at% Cu of the ISS comparison. This is a much better agreement than what would have resulted from using the sensitivity factors as determined in a different experimental setup. Also, realizing that the absolute composition determination is usually not better than ±5 at% due to the uncertainty in the estimation of $n_{i,ref}$ of the reference samples, the accuracy as obtained using this in situ calibration procedure is quite acceptable. Using well-ordered single-crystal reference samples could give even more accurate quantitative results due to the better definition of $n_{i,ref}$.

4. Discussion and summary

When discussing the results of the round robin experiment several aspects have to be considered. For example, all the instruments used are essentially 'home-built' instruments, not commercially available systems. Furthermore, in very few cases were the measurements repeated after the first round or were additional measurements taken (Firenze and Louvain). That means, practically all results are completely unbiased with respect to each other. The reason for no additional measurements is obvious, they are time consuming. As shown in Fig. 2, it took Osnabrück more than two weeks to clean the Al, it then takes only hours to measure the full set of energy spectra. With the other targets the procedure is faster. Without a target transfer system or the possibility to hold more than 1 target at a time in the target manipulator, time is also lost for pumping and baking. Not all systems used afford these facilities. An additional

aspect is the fact that most of the systems used are not 'devoted' LEIS systems. In many cases LEIS is an additional facility to check target composition or simply cleanliness, but then go on to other types of experiments. In a way, only the Eindhoven and the Garching experiments are 'devoted' LEIS systems.

In summarizing the outcome of the round robin experiment we list here the most important findings and requirements for a successful, quantitative LEIS analysis. Besides the proper basic equipment and well trained personnel, a calibration standard is needed. Any well cleaned metal can serve for that purpose. However, out of the metals tested here, Al, Ni, Cu, Pd and Pt, Cu is the most favourable material. Al is relatively hard to clean, and Ni, Pd and Pt tend to contaminate faster then Cu, due to the higher reactivity of this group of metals compared to Cu. But it may adsorb contaminants from the residual gas, thus lowering the backscattered ion yield. Experimental problems arise from the control of the primary ion beam, its size and its position on the target relative to the target area seen by the energy analyser. There are no simple means to check the size and/or the current density profile of a low energy ion beam. Fluorescent screens do not work. One solution of the task is the use of a small aperture, moveable Faraday cup. Channel plate detectors coupled to a position sensitive detector can only be used at very low beam currents (<pA) [18]. When increasing the beam current, the beam profile may change. Beam imaging at higher current densities is possible using secondary electron emission (SEE). Even though the SEE-coefficients are low (of the order of 0.15–0.3 e/ion in the energy range used here) imaging is possible and used e.g. in Osnabrück and Eindhoven. By this means at about 2 keV the primary beam can be focused qualitatively – without control of the beam current density distribution – and the scanning area for the sputtering is set. In Eindhoven a beam position analyser (BPA) is used consisting of a channeltron detector behind a small diaphragm. The little instrument can be moved with the target manipulator over the beam spot, thus affording good control of the primary beam. For any laboratory setting up a LEIS system for quantitative analysis the results presented here may give a guideline how to set up the experiment and the procedure of calibration.

The results show no new problems with respect to the ion survival probability beyond previously published data [1–4,13,14,16] and references therein. Therefore the results concerning the ion survival from this study are not discussed here.

Acknowledgements

The study was financially supported by the EU within the program Human Capital & Mobility (HCM) CHRX-CT94–0479. Osnabrück is grateful for support by the Deutsche Forschungsgemeinschaft (DFG).

References

[1] H. Niehus, W. Heiland, E. Taglauer, Surf. Sci. Repts. 17 (1993) 213.
[2] E. Taglauer, Ion spectroscopies for surface analysis, in: A.W. Czanderna, D.M. Hercules (Eds.), Meth. of Surf. Characterization series, Plenum Press, New York, 2, 1991, p. 363.
[3] H.H. Brongersma, G.C. van Leerdam, Fundamental aspects of heterogeneous catalysis studied by particle beams, in: H.H. Brongersma, R.A. van Santen (Eds.), NATO ASI series B 265, 1991, p. 283.
[4] H.H. Brongersma, P.A.C. Groenen, J.-P. Jacobs, Science of Ceramic Surfaces II, in: J. Nowotny (Ed.), Elsevier, Amsterdam, 1994, p. 113.
[5] S. Tougaard, J. Vac. Sci. Tech. A8 (1990) 2197.
[6] M. Schleberger, D. Fujita, C. Scharfschwerdt, S. Tougaard, Surf. Sci. 357/358 (1996) 302.
[7] H. Oechsner, J. Mass. Spectr. and Ion Proc. 143 (1995) 271.
[8] A. Benninghoven, F.G. Rüdenauer, H.W. Werner, Secondary Ion Mass Spectrometry, Wiley, New York, 1987.
[9] H.H. Brongersma, N. Hazewindus, J.M. van Nieuwland, A.M.M. Otten, A.J. Smets, Rev. Sci. Instr. 49 (1978) 707.
[10] L. Houssiau, P. Bertrand, Nucl. Instr. and Meth. B 118 (1996) 467.
[11] B. Baretzky, IPP-Report 9/53 (1985).
[12] M. Galeotti, B. Cortigiani, V. Bardi, J. Electr. Spectr. and Rel. Phen. 76 (1995) 91.
[13] J. Möller, K.J. Snowdon, H. Niehus, W. Heiland, Surf. Sci. 178 (1986) 475.
[14] J.-P. Jacobs, S. Reijne, R.J.M. Elfrink, S.N. Mikhailov, H.H. Brongersma, J. Vac. Sci. Tech. A 12 (1994) 2308.

[15] R. Souda, M. Aono, Nucl. Instr. and Meth. B, 15 (1986) 114; T.M. Thomas, H. Neumann, A.W. Czanderna, J.R. Pitts, Surf. Sci. 175 (1986) L737.
[16] E. Taglauer, Appl. Phys. A 3 (1985) 161.
[17] S.N. Mikhailov, R.J.M. Elfrink, J.-P. Jacobs, L.C.A. van Oetelaar, P.J. Scanlon, H.H. Brongersma, Nucl. Instr. and Meth. B 93 (1994) 149.
[18] A. Niehof, W. Heiland, Nucl. Instr. and Meth. B 48 (1990) 306.